Adsorption and Desorption of H2 on Graphite by Molecular Dynamics Simulations

ARTICLE *in* THE JOURNAL OF PHYSICAL CHEMISTRY C · MAY 2010

Impact Factor: 4.77 · DOI: 10.1021/jp1011022

3 AUTHORS, INCLUDING:

Jean-Marc Simon
University of Burgundy
83 PUBLICATIONS **673** CITATIONS
SEE PROFILE

Signe Kjelstrup
Norwegian University of Science and Tech…
316 PUBLICATIONS **3,666** CITATIONS
SEE PROFILE

Adsorption and Desorption of H_2 on Graphite by Molecular Dynamics Simulations

J.-M. Simon,*,† O.-E. Haas,‡ and S. Kjelstrup‡,§

Laboratoire Interdisciplinaire Carnot de Bourgogne, UMR-5209 CNRS-Université de Bourgogne, 9 av. A. Savary, 21000 Dijon, France, Department of Chemistry, Norwegian University of Science and Technology, Trondheim, NO 7491 Trondheim, Norway, and Department of Process and Energy, Technical University of Delft, 2628 EV Delft, The Netherlands

Received: February 4, 2010; Revised Manuscript Received: April 30, 2010

We report equilibrium properties and rate constants for adsorption and desorption of hydrogen on graphite as a function of temperature, from 70 to 390 K, using equilibrium molecular dynamic simulations. Below 170 K, we found that isotherms can be modeled with Langmuir isotherms, while at higher temperature, Henry's law applied. The isosteric adsorption enthalpies and entropies were calculated for different loadings and showed a decrease as the loading increased, compatible with a nonideal adsorbate. These results are in good agreement with previous results from the literature. The observed adsorption and desorption rate constants were, however, not described by Langmuir kinetics. We propose a set of rate equations which follow from the law of mass action with activities as variables rather than concentrations. The unidirectional rates combine at equilibrium to give the Langmuir isotherm with the same result for the Langmuir constant. This kinetic behavior is interpreted as the consequence of a mobile adsorbed phase. The effect may be important for fuel cell performance or hydrogen storage in carbonaceous materials.

Introduction

Despite the fact that the study of adsorption−desorption kinetics goes back more than hundred years,[1,2] the field remains active, probably because reactions and transport phenomena at surfaces are essential to many industrial or natural processes.[3−6,6−11] Adsorption rate expressions, similar to chemical reaction rates, can be grouped in two broad categories: kinetic and thermodynamic.

Kinetic theories view the process by the probabilities for collision[2] and express the law of mass action[1] with rate constants and concentrations. A famous example is the Langmuir model.[12] This model gives the adsorption rate as proportional to the gas pressure and to the surface free space, while the desorption rate depends on the surface coverage only.

Ward and co-workers[3−7] developed statistical rate theory after the 1980's from a thermodynamic and quantum mechanics starting point. They consider the probability for mass exchange between two states in terms of their difference in entropy. Kreuzer and co-workers[8,13−18] used nonequilibrium statistical thermodynamics and developed rate expressions from the statistical lattice-gas model. Many experiments, like temperature-programmed desorption[6,8,9,15] or sorption experiments with different sorbents[10] have been successfully described by these theories. The choice of one equation instead of another one is not trivial, however; see Ho et al.[10]

In this context and despite the work of Kreuzer and co-workers,[8,13−18] it is fair to say that nonequilibrium thermodynamics[19] has not been popular. This theory gives a relation for the net rate of adsorption and its driving force which is linear. The theory has been used to describe transport phenomena in homogeneous systems and has now been extended to heterogeneous systems,[20] as well as to the mesoscopic level.[21] The extension to processes on the mesoscopic level, like chemical reactions, is promising, because this enables one to deal with these in a realistic manner. Their flux−force relations are nonlinear under realistic conditions. The theory is compatible with the law of mass action,[21] which is vital for its application. An interesting point follows. The net rate of adsorption becomes a function of component activities rather than concentrations.[13]

It is therefore interesting to pursue this point: are there cases of adsorption/desorption where activities must be used in the rate equations, rather than concentrations? And, can this change of focus lead to a better understanding of the processes that take place? If the answer is yes, rate equations derived from a thermodynamic basis may deserve more attention. It is the aim of this article to present an example of such a case.

The physisorption of hydrogen on a graphite surface is a reversible, simple reaction that is suitable for analysis of the theoretical problem posed above. The system can be exactly modeled and monitored.[22−24] It is also of practical importance. A lot of attention is now given to the problem of hydrogen storage on graphite and graphene.[25,26] We have therefore chosen to study hydrogen adsorption on a graphite surface as an example system.

We shall see that the system is well-characterized, in agreement with literature data, by isotherms, isosteric enthalpies, and entropies of adsorption. The Langmuir equilibrium constant is determined, but the desorption and adsorption rates are proportional to the surface and gas activities, and do not follow Langmuir kinetics. This can add to our understanding of the state of hydrogen molecules at the surface. It may also contribute to the field of reaction kinetics.

Molecular dynamics simulations are excellently suited to investigate the type of problems described above. The advantages of molecular dynamic simulations are that macroscopic behavior can be directly connected to molecular behavior and that there is no bias toward a particular macroscopic description. For instance, we have tested the validity of the underlying

* To whom correspondence should be addressed. E-mail: jmsimon@u-bourgogne.fr.
† Université de Bourgogne.
‡ Norwegian University of Science and Technology, Trondheim.
§ TU Delft.

10.1021/jp1011022
Published on Web 05/14/2010

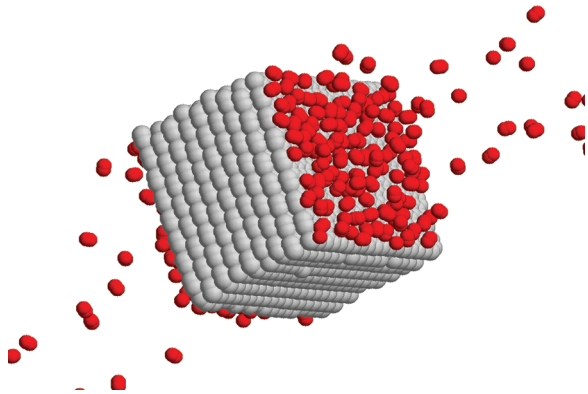

Figure 1. Snapshot of an equilibrium configuration of crystalline graphite at 90 K and two adjacent gas phases. The carbon atoms are painted light gray and the hydrogen atoms are red. Hydrogen molecules are adsorbed on the graphite surface. There is equilibrium between the adsorbed layer and the gas phase.

assumptions in nonequilibrium thermodynamics using molecular dynamics simulations; see ref 20 for literature.

The rate of desorption and adsorption will thus be investigated here with molecular dynamics simulations. Interpretation in terms of the classical Langmuir model and a thermodynamically based rate equation are then possible. We shall see that the first description fails to model the unidirectional rates in the equilibrium exchange situation, while the last description is good and leads to a different understanding of the adsorption process.

Equilibrium Exchange Rates

The surface in our system is positioned between the gas phase and the graphite phase (see Figure 1). The reaction between the gas phase and the adsorbed phase on the surface can be written

$$H_2(g) \rightleftharpoons H_2(ads) \tag{1}$$

At equilibrium, the gas chemical potential is equal to the surface chemical potential

$$\mu^g = \mu^s \tag{2}$$

where μ^s is the chemical potential of hydrogen in the surface.

Hydrogen molecules are physisorbed on the graphite. They can move along the surface and leave it.[27] This generates adsorption and desorption fluxes, J_a and J_d, respectively. The net rate

$$J = J_a - J_d \tag{3}$$

is zero at equilibrium.

Different expressions for the rate of adsorption and desorption are available, depending on the condition of the adsorbed molecule: mobile−nonmobile, chemisorbed−physisorbed, cf. refs 3−10, 16−18, 28−32. We have chosen a central model with which to compare: the Langmuir model.[12] In the Langmuir model, the adsorption sites are fixed and energetically equivalent, and the adsorbed molecules do not interact with each other.[12] Under these conditions, the forward rate, J_a, is proportional to the gas pressure, p, and the vacant space on the surface $(1 - \theta)$, where θ is the surface coverage or the ratio between the actual surface concentration, c^s, and the concentration at saturation, c^{sat} ($\theta = c^s/c^{sat}$). The desorption rate J_d is simply proportional to the surface coverage

$$\begin{aligned} J_a &= k_a^L \frac{p}{p^0}(1 - \theta) \\ J_d &= k_d^L \theta \end{aligned} \tag{4}$$

In these expressions, k_a^L and k_d^L are the rate constants for adsorption and desorption in the Langmuir model. At equilibrium, the fluxes are equal, giving the Langmuir equilibrium constant $K_L = k_a^L/k_d^L$, and the Langmuir isotherm (cf. eq 10). We shall see below (Figure 8) that eq 4 fails to describe the unidirectional rates for this system.

The rate equation predicted from mesoscopic nonequilibrium thermodynamics[21] is nonlinear in the driving force, while classical nonequilibrium thermodynamics give a linear relation. The equilibrium condition is always eq 2. By introducing the expressions for the chemical potentials below (eqs 9, 10), we can rewrite the condition as

$$a^g \exp\left[\frac{\mu^0}{RT}\right] = a^s \exp\left[\frac{\mu^*}{RT}\right] \tag{5}$$

where a^g and a^s are the activities in the gas phase and the adsorbed phase, respectively, and μ^0 and μ^* are the corresponding standard states. At equilibrium, when $J_a = J_d$, we may therefore also write

$$\begin{aligned} J_a &= k_a^a a^g \\ J_d &= k_d^a a^s \end{aligned} \tag{6}$$

where k_a^a and k_d^a are rate constants for adsorption and desorption, where each contain an Arrhenius factor with the standard state chemical potential. The unidirectional adsorption and desorption rates are now directly proportional to the activities. We shall see that hydrogen adsorption on graphite can best be described by eq 6. The physical model behind the Langmuir equation is therefore not the best explanation for the physisorption of hydrogen on graphite. We shall speculate that this comes from the fluidlike layer of hydrogen on the surface, with highly mobile molecules.

Thermodynamic Relations. The thermodynamic relations needed to describe the data are standard.[33] In all simulated cases, we verified that the assumption of ideal gases is fulfilled. The chemical potential of the gas, μ^g, is therefore

$$\mu^g = \mu^0 + RT \ln \frac{p}{p^0} \tag{7}$$

Here, μ^0 is the standard chemical potential at pressure $p^0 =$ 1 bar and p is the actual gas pressure, meaning that $a^g = p/p^0$ in eq 6.[33] For the surface, we have

$$\mu^s = \mu^* + RT \ln a^s \tag{8}$$

where μ^* is the chemical potential with Henry's law standard state and $a^s = (\gamma c^s)/c^*$ is the surface activity. Here, c^s is the surface molar concentration (given in mol/m^2) and c^* is the unit concentration of the hypothetical standard state.

From the equations (eqs 2, 7, and 8), we first obtain the equilibrium constant K_H

$$K_H = \frac{c^s \gamma}{c^*} \frac{p^0}{p} \tag{9}$$

where K_H can be found as Henry's law constant at low surface concentrations (when $\gamma = 1$). The activity coefficient γ measures the deviation from Henry's law.

The Langmuir equilibrium constant K_L is now from eq 4

$$K_L = \frac{\theta}{(1-\theta)} \frac{p^0}{p} \tag{10}$$

By equating the two, we see that

$$\gamma = \frac{1}{1-\theta} \tag{11}$$

when the definition $\theta = c^s/c^{sat}$ is used. When Langmuir's isotherm model applies, the relation between the equilibrium constants is then

$$K_L = K_H \frac{c^*}{c^{sat}} = K'_H \tag{12}$$

where the right-hand side equality defines K'_H.

We can solve eq 10 for the fractional coverage θ and obtain

$$\theta = \frac{K_L \frac{p}{p^0}}{1 + K_L \frac{p}{p^0}} \tag{13}$$

We shall obtain K_L and c^{sat} by fitting the simulation data to the Langmuir model using this equation. The parameters are functions of the temperature and the adsorbate/adsorbent interaction. We shall calculate K'_H from data for the region where Henry's law applies, while γ shall be directly obtained from the simulation data as a correction factor to Henry's law. The results shall next be compared with the Langmuir condition, eq 11.

Given the expressions of the activities above, the expressions for the adsorption and desorption rates to be tested, eq 6, are

$$\begin{aligned} J_a &= k_a^a \frac{p}{p^0} = k_a \frac{p}{p^0} \\ J_d &= k_d^a \frac{c^s}{c^*} \gamma = k_d \theta \gamma \end{aligned} \tag{14}$$

In this expression, $k_d = k_d^a c^{sat}/c^*$ and $k_a = k_a^a$. At equilibrium, when $J_a = J_d$, we see that the combination of these equations gives the Langmuir isotherm with $K_L = k_a/k_d$ and $\gamma = 1/(1-\theta)$.

Simulation Details

The Simulated System. The equilibrium molecular dynamics (EMD) system was built of an infinite sheet of crystalline graphite in contact with hydrogen molecules, H_2. The graphite has a hexagonal crystallographic structure with space group $P6_3/mmc$ without any defects. The crystal is made from 9 sheets of graphene and contains 5184 carbon atoms. Following the crystallographic structure, the graphene sheets are oriented in our simulation box such that the surfaces of the sheets are perpendicular to the z direction. The size of the crystal is 44.208 Å and 34.0313 Å in x and y directions, respectively, and about 30 Å in the z direction.[34] Periodic boundary conditions are applied in x and y directions in the limits of the crystal and in the z direction at 95.254 Å from the center of the crystal. This symmetry gives in effect an infinite succession of two infinite graphite crystal surfaces separated by a gaseous zone of about 160 Å in the z direction, where the H_2 molecules are located.

TABLE 1: Parameters Used in the Simulation[22−24,35a]

Lennard-Jones	
hydrogen	graphite
$\varepsilon = 27.655$/K $\sigma = 2.63984$ /Å	$\varepsilon = 25.89$/K $\sigma = 3.34380$ /Å
stretching	
hydrogen, Morse	graphite, harmonic
$D_e = 458.0$/kJ/mol $a = 1.946$ /Å $^{-1}$ $r_0 = 0.7414$ /Å	$k_S = 4393.9$/kJ/mol $r_0 = 1.42$ /Å
graphite	
bending	torsion
$k_{3B} = 418.2$/kJ/mol/rad^2 $\theta_0 = 120$/degrees	$k_T = 26.15$/kJ/mol

[a] For explanation of symbols, see text.

Five different systems were simulated to investigate the kinetics of adsorption/desorption as a function of surface concentration. The surface concentration variation was implemented by simulating with five different global densities. The five different numbers of hydrogen molecules were $N_{H_2} = 50$, 100, 150, 200, and 300. For each N_{H_2}, simulations were preformed at seventeen different temperatures, ranging from 70 to 390 at 20 K intervals. Additional simulations with $N_{H_2} = 10$ were performed at 70, 90, 110, 150, 170, 190, and 230 K to investigate the behavior of the systems at low density and low temperature. This gave a total of 85 simulations describing the dynamics on the graphite surface as a function of surface concentration and temperature.

Atomic and Molecular Interactions. The model is based on an atomic description of the graphite and hydrogen. The atoms interact through intermolecular and intramolecular potentials. The intramolecular potentials are given in ref 24, Table 1, and eqs 2−4. The intermolecular potential is the Lennard-Jones potential.[35] The parameters for the Lennard-Jones potential are taken from the MM2 force field,[23] while the parameters of the intramolecular potentials come from the DREIDING force field[22] for graphite and the Delft Molecular Mechanics (DMM) force field[24] for the hydrogen molecules. The parameters of these potentials were fitted to give good agreement with experimental physical properties of a large variety of compounds, mainly those including carbon and hydrogen, like hydrocarbons. No quantum effect was added like those incorporated through a Feynman-Hibbs variational approach. On the basis of the work of Anil Kumar et al.,[36] it is reasonable to believe that the quantum corrections are negligible at the simulated temperatures.

To describe the stretching of bonds, a Morse potential was used for hydrogen and a harmonic potential for graphite. The Morse potential, V_M, was

$$V_M(r_{ij}) = D_e\{1 - \exp[-a(r_{ij} - r_0)]\}^2 \quad (15)$$

where D_e, r_0, and a are the input parameters of the potential and r_{ij} is the distance between atom i and j. The harmonic carbon−carbon stretching potential, V_S was

$$V_S(r_{ij}) = \frac{1}{2} k_S(r_{ij} - r_0)^2 \quad (16)$$

where k_S is the force constant.

Graphite bending was calculated using a harmonic potential. The bending potential, V_B, was

$$V_B(\theta_{ijk}) = \frac{1}{2} k_B(\theta_{ijk} - \theta_0)^2 \quad (17)$$

In this equation, θ_{ijk} is the angle between the three atoms i, j, and k; k_B is the force constant; and θ_0 is the angle giving minimum energy.

Torsion in graphite was described by the following potential equation

$$V_T(\omega_{ijk}) = \frac{1}{2} k_T[1 - \cos(2\omega)] \quad (18)$$

Here, ω is the torsion angle, and k_T is the force constant.

Nonbonded potentials V_{nb} were applied between hydrogen and carbon atoms, hydrogen atoms belonging to different molecules, and between carbon atoms in different graphene sheets or separated by more than three bond lengths within the same graphene sheet. The nonbonded potential was given by a shifted and truncated 12−6 Lennard-Jones (LJ) type potential

$$V_{LJ}(r_{ij}) = 4\varepsilon_{ii}\left[\left(\frac{\sigma_{ij}}{r_{ij}}\right)^{12} - \left(\frac{\sigma_{ij}}{r_{ij}}\right)^{6}\right] \quad (19)$$

$$V_{nb}(r_{ij}) = \begin{cases} V_{LJ}(r_{ij}) - V_{LJ}(r_C) & r_{ij} \le r_C \\ 0 & r_{ij} > r_C \end{cases} \quad (20)$$

Here, r_{ij} is a distance between atoms i and j, ε_{ij} and σ_{ij} are LJ potential parameters, and r_C is the cutoff radius equal to 2.5 σ_{CC}. The LJ interaction parameters between different types of atoms are calculated from the Lorentz−Berthelot mixing rules[35]

$$\varepsilon_{ij} = \sqrt{\varepsilon_{ii}\varepsilon_{jj}} \quad (21)$$

$$\sigma_{ij} = \frac{1}{2}(\sigma_{ii} + \sigma_{jj}) \quad (22)$$

All the potential parameters are summarized in Table 1.

Simulation Procedures. The dynamics were obtained by integrating Newton's equations of motion using the velocity Verlet algorithm.[35] All simulations had time steps of 0.001 ps. The initial configuration was constructed by randomly distributing the H_2 molecules in the gas phase. Molecules were located such that they do not overlap with each other or the graphite crystal. The system was stabilized during 400 ps by fixing the temperature at an imposed value using a simple rescaling of the velocities. When the system was in thermal equilibrium, the conditions of the simulations were changed to those of a microcanonical ensemble (constant energy). Trajectories of 1700 ps were then computed and analyzed. Variables were calculated every 10 time steps, averaged over 1 ps, and stored.

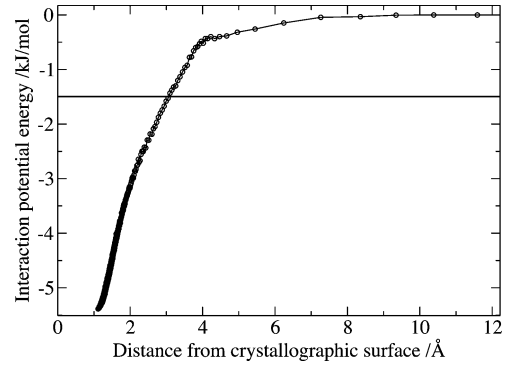

Figure 2. Average potential energy of a hydrogen molecule at 70 K as a function of distance from the surface of the graphite. The solid line marks the boundary d, which defines whether a hydrogen molecule is adsorbed or not.

Calculated Variables

Surface Concentration. The surface concentration c^s is defined as the averaged number of molecules adsorbed divided by the surface area and the Avogadro number. The procedure to decide whether a molecule is adsorbed or not is based on an energetic criterion.

The mean interaction potential energy between a hydrogen molecule and the graphite sheet at 70 K is plotted as a function of distance from the crystallographic surface (z) in Figure 2. The interaction potential energy is calculated separately for each molecule along its trajectory as the sum of all contributions with the graphite sheet within the cutoff radius, using eq 20; it is then sorted out as a function of the distance from the graphite sheet and averaged.

The potential energy is zero in the gas phase and decreases to a minimum of −6 kJ/mol when the molecule is adsorbed. If the potential energy of a molecule is lower than −1.5 kJ/mol, below the line in Figure 2, a hydrogen molecule is defined as adsorbed. This gives an energy criterion for finding the surface concentration c^s. This criterion is somewhat arbitrary, so in order to investigate the influence of the criterion on the results, we performed a systematic study (not shown here) changing the criterion. The conclusions that we reached in this paper were always verified.

Temperature Calculation. The kinetic temperature, T, was obtained by combining two definitions of the internal kinetic energy, K, one coming from the equipartition of the energy and the second from the kinetic energy of the simulated particles

$$K = \frac{1}{2}(3N_{at} - 6)k_B T = \frac{1}{2}\sum_{i=1}^{N_{at}} m_i\langle|\mathbf{v}_i - \mathbf{v}|^2\rangle \quad (23)$$

At the left-hand side of this equation, N_{at} is the total number of atoms of the system, $3N_{at} - 6$ is total number of degrees of freedom of the system, k_B is the Boltzmann constant, and T the temperature. At the right-hand side, $\mathbf{v}_i$ is the instantaneous velocity of the atom i and mass m_i, and $\mathbf{v}$ is the barycentric instantaneous velocity.

Pressure Calculation. The gas pressure, P, was obtained using the perfect gas law

$$PV_{gas} = N_{gas}k_BT \quad (24)$$

where N_{gas} and V_{gas} are the number of molecules located in the gas phase and the volume of the gas phase, respectively. A molecule is located in the gas phase if its interaction energy with the graphite is higher than −0.5 kJ/mol (see Figure 2). By calculating separately the compressibility, we verified that it was equal to 1 within the statistical uncertainties for all cases.

Rates of Adsorption and Desorption at Equilibrium. The rate of adsorption was calculated at equilibrium as the average number of molecules per unit time per unit area being adsorbed and coming from the gas phase. The unidirectional flux in the opposite direction, the desorption rate, was calculated as the average number of molecules per unit time and unit area entering the gas phase and coming from the adsorbed phase. From these definitions, the rates were positive, and the net flux J was calculated as the difference between the adsorption and the desorption rates.

Results and Discussion

We first present results for the general thermodynamic properties of the system, to show that these are fully compatible with results reported by others[37−41] and modeled well by the common Langmuir equation. The unidirectional rates and their dependence on pressure and surface concentration or activity are next presented and discussed.

Thermodynamic Properties. The isotherms plotted from the surface concentration and the corresponding pressure are shown in Figure 3 for temperatures between 70 and 390 K. The Langmuir eq 13 was fitted to simulated data between 70 and 170 K, and we found c^{sat} and K_L as a function of temperature. The Henry eq 9 was fitted, using extrapolated values of c^{sat} and $\gamma = 1$ to data simulated between 190 and 390 K to give K'_H. The results, given in Table 2, for c^{sat} and $K'_H = K_L$ gave

$$c^{sat} = c_0 \exp\frac{-E_{sat}}{RT} = 1.35 \times 10^{-2} \exp\left(\frac{180\ \text{J/mol}}{RT}\right)$$
$$K'_H = K_0 \exp\frac{-E_{eq}}{RT} = 1.72 \times 10^{-4} \exp\left(\frac{6000\ \text{J/mol}}{RT}\right) \quad (25)$$

The unit of c_{sat} is given in mmol/m^2. From these relations, K_H follows.

As seen from Figure 3, the Langmuir isotherm fits the data from 70 to 170 K very well, and so does Henry's law above this temperature. Similar trends were observed by Benard et al., Hirscher et al., Panella et al., and Zhou et al.[37−40] We can compare the amount of maximum adsorbed H_2 in mol/m^2 at 70−77 K. Our results give 1.85×10^{-5} mol/m^2, while the values of the experimental papers are in the range of 8.93×10^{-6} to 5.62×10^{-5} mol/m^2. So, our results are within the range of experimental values.

From these values, we found the activity coefficients as given by eqs 9 and 11. The results are plotted in Figure 4. Both sets of data are in good agreement, although values obtained by eq 11 are on the whole somewhat larger than the values found from eq 9.

The natural logarithm of p/p^0 was plotted for a given surface concentration, against the inverse of the temperature in Kelvin in Figure 5. The pressure in each case was calculated from the Langmuir equation, using parameters in Table 2. This gives the isosteric plot as defined by eq 26. From these plots, we found

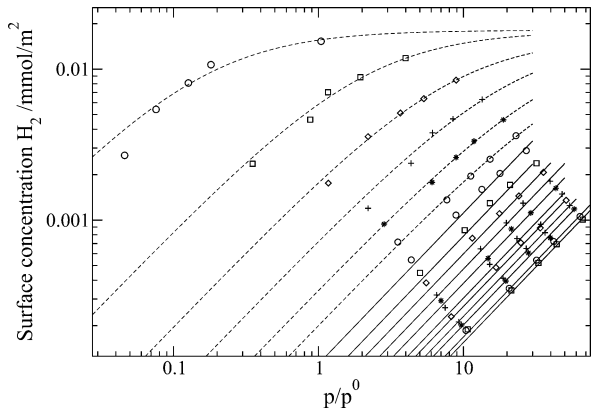

Figure 3. Data points from the simulations fitted to Langmuir isotherms (dotted lines) and Henry isotherms (full lines). The temperature decreases from 70 K at the top left to 390 K at the bottom right.

TABLE 2: Equilibrium Parameters Found from the Simulation Data[a]

temperature/Kelvin	c^{sat}/mmol/m^2	$K'_{H,isotherms}$	$K'_{H,rates}$
70	0.0181	6.14	5.05
90	0.0179	0.485	0.530
110	0.0163	0.124	0.126
130	0.0161	4.68×10^{-2}	4.67×10^{-2}
150	0.0157	2.23×10^{-2}	2.26×10^{-2}
170	0.0154	1.34×10^{-2}	1.29×10^{-2}
190	0.0151	7.36×10^{-3}	8.32×10^{-3}
210	0.0150	5.23×10^{-3}	5.83×10^{-3}
230	0.0148	4.03×10^{-3}	4.34×10^{-3}
250	0.0147	3.22×10^{-3}	3.39×10^{-3}
270	0.0146	2.61×10^{-3}	2.75×10^{-3}
290	0.0146	2.09×10^{-3}	2.29×10^{-3}
310	0.0145	1.85×10^{-3}	1.96×10^{-3}
330	0.0144	1.60×10^{-3}	1.70×10^{-3}
350	0.0144	1.41×10^{-3}	1.51×10^{-3}
370	0.0143	1.18×10^{-3}	1.35×10^{-3}
390	0.0143	1.08×10^{-3}	1.22×10^{-3}

[a] $K'_{H,isotherms}$ are the results found by using eq 13 in the 70−170 K range and eq 12 in the 190−390 K range. $K'_{H,rates}$ are the results found by using eq 14 and the fit in Figure 10.

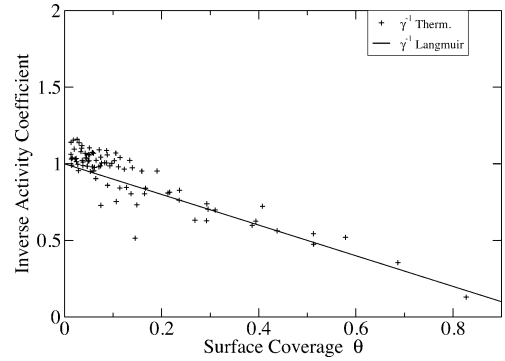

Figure 4. Inverse activity coefficient vs surface coverage. Values from eq 11 give the full line. The values calculated using eq 9 are shown by +.

the isosteric enthalpy of adsorption $\Delta_{ads}H$ from the slope and the isosteric entropy of adsorption $\Delta_{ads}S$ from the intercept

$$\ln\left[\frac{p}{p^0}\right]_{cs} = \frac{\Delta_{ads}H}{RT} - \frac{\Delta_{ads}S}{R} \quad (26)$$

The straight lines mean that the enthalpy of adsorption can be regarded as a negligible function of temperature. The

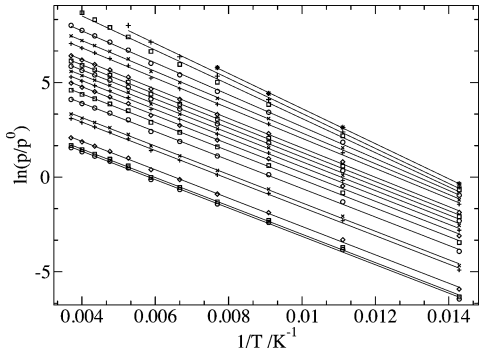

Figure 5. Adsorption isosteres for 19 surface concentrations (in mmol/m^2). The slope of one fitted line gives the heat of adsorption and the intercept gives the entropy of adsorption for one concentration.

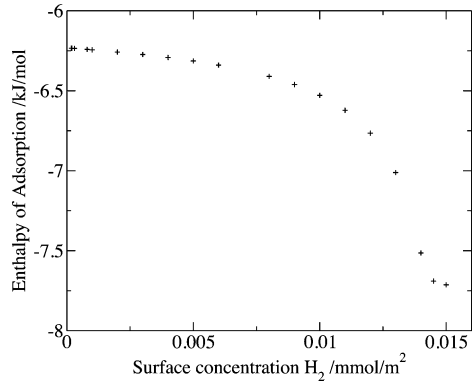

Figure 6. Isosteric enthalpy of adsorption as a function of surface concentration.

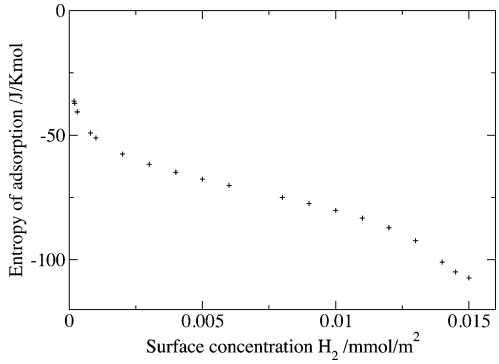

Figure 7. Isosteric entropy of adsorption as a function of surface concentration.

results for the isosteric enthalpy and entropy of adsorption are plotted in Figure 6 and Figure 7. The values in both plots are changing with surface concentration. Both decrease with increasing surface concentration toward a minimum around 0.015 mmol/m^2. The isosteric enthalpy varies between −6.0 and −7.7 kJ/mol, in agreement with the physisorption reported previously,[41] and it is almost constant until 0.01 mmol/m^2. Above 0.01 mmol/m^2, the value starts to decrease rapidly until the surface concentration approaches 0.0145 mmol/m^2. At this value, the isosteric enthalpy apparently reaches the lowest value, −7.7 kJ/mol. The isosteric entropy has a rapid decrease below 0.0025 mmol/m^2 starting from a value of about −30 J/K/mol and decreases next linearly with the surface concentration until 0.011 mmol/m^2. Then, the value of the isosteric entropy drops to its lowest value, approximately −110 J/K mol, at 0.015 mmol/m^2. The effect of the concentration is much more noticeable on the value

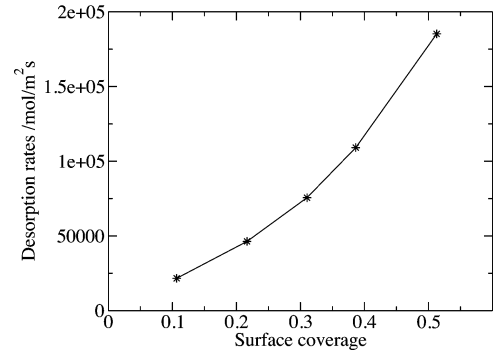

Figure 8. Desorption rate at 110 K as a function of surface coverage. The trend is not a linear function of the coverage, contrary to the Langmuir model.

of the entropy, 300% of change, than on the enthalpy, 30% of change, indicating large entropic effects on the surface.

We conclude this section by stating that the system has characteristic properties for physisorption and can be described well by Langmuir isotherms, in agreement with others.[37−41]

Equations for Unidirectional Rates. We report now on the kinetic observations, and show that the unidirectional rates do not obey the Langmuir model.

The desorption rate at a temperature of 110 K was plotted as a function of the surface coverage in Figure 8. At low coverage, the rate increased linearly and according to the Langmuir model. At higher densities, however, it increased more rapidly, for all temperatures investigated. As a consequence, k_a^L and k_d^L, cf. eq 4, are not constant with the surface coverage, as seen in Figure 9a for different temperatures. The ratio between the Langmuir adsorption and desorption rate constants are constant, however, so the equilibrium constant K_L is then constant with the surface coverage, as expected.

The value of the rate constants k_a and k_b, cf. eq 14, are shown as a function of the surface coverage in Figure 9b. They are within statistical uncertainty independent of the surface coverage for a given temperature. These results show that eqs 14 are valid for this system within the investigated temperature and pressure ranges. We also verified that these equations are valid independent of the criterion used to define if a molecule is adsorbed or not.

As can be seen in Figure 10, the values of k_a and k_d decrease and increase, respectively, as a function of the temperature following an exponential law

$$k = k_0 \exp\left(\frac{-E}{RT}\right)$$

The natural logarithm of the rate constants versus the inverse of the temperature gives the apparent activation energy E as the slope and the pre-exponential parameters as the intercept k_0. To get better statistics, we used the average value from each temperature as an estimate as seen in Figure 10 (the lines). The results are

$$k_a = 3.5 \times 10^3 \exp\left(\frac{1500\ \text{J/mol}}{RT}\right)$$
$$k_d = 1.8 \times 10^7 \exp\left(\frac{-4400\ \text{J/mol}}{RT}\right) \quad (27)$$

The units of the activation energy and of the constant are, respectively, J/mol and mol/m^{2}s. The negative adsorption energy

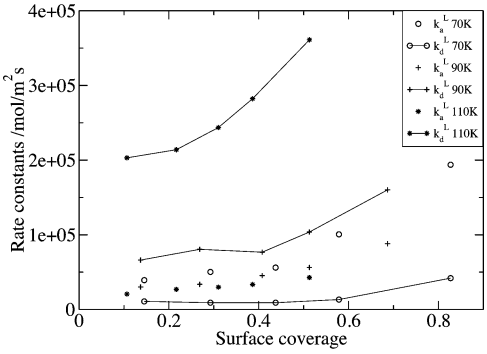

(a) Langmuir model

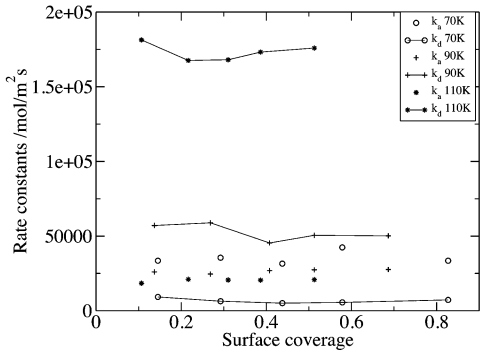

(b) Our model

Figure 9. (a) Langmuir rate constants as calculated from eq 4 as function of the surface coverage for 70−110 K. They are not constant with surface concentration as expected from Langmuir kinetic model. (b) Rate constants as calculated from eq 14 as a function of the surface coverage for 70, 90, and 110 K. They are constant with surface concentration.

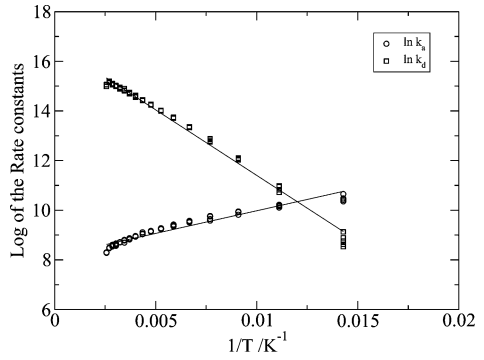

Figure 10. Logarithm of the rate constants as function of the inverse of temperature.

is typical for systems with weak physical adsorption, and also weakly exothermic reactions, according to Henriksen and Hansen.[42]

From the ratio k_a/k_d, we calculated the equilibrium constant K'_H. The values of K'_H are presented in Table 2. By plotting the natural logarithm of K'_H vs the inverse of the temperature, we found the temperature dependence as

$$K'_H = 1.9 \times 10^{-4} \exp\left(\frac{5900\ \text{J/mol}}{RT}\right)$$

which is in agreement with the equilibrium constant found from the isotherms, cf. eq 25. This means that the model is thermodynamically consistent.

Surface with Mobile Gas Molecules. The rate equations from the Langmuir model eq 4 and the alternative eq 14 give the same expression for the equilibrium constant, but they give different physical pictures of the kinetics of adsorption and desorption.

We have found that the rate of adsorption depends only on the temperature and the gas pressure as described by eq 14. It is not proportional to the free space on the surface as predicted by Langmuir's kinetics. This somewhat unexpected behavior must mean that one or more of the assumptions behind the Langmuir model are not valid. In the Langmuir model, one assumes for instance that the adsorbate is bound to particular sites, with the same binding energy.

We have previously seen, from experiments as well as simulations, that the diffusion coefficient for transport of hydrogen along the graphite surface has a magnitude that is common in fluids, between 10^{-8} and 10^{-6} m^2/s.[27] A large surface diffusion coefficient means that the adsorbed phase is mobile, not stuck in space. Therefore, at the temperatures in question, the molecules cannot be considered as trapped on specific adsorption sites. They can move very easily along the surface, even a few angstroms up above the graphite. As a consequence, adsorption can take place independent of the availability of vacant sites. Therefore, the adsorption rate becomes only a function of the gas pressure.

A physical explanation of the desorption rate is less clear. The molecules desorb with a rate that is proportional to the surface coverage. This part is expected, but the desorption is also seemingly inversely proportional to the free space. In the regime where Henry's law applies, the effect is not significant. Close to saturation, when the pressure is high, a relatively large increase in the pressure has a small influence on the number of adsorbed molecules. The term $k_d\theta$ is then nearly constant. A remaining factor must then account for the increase in the unidirectional rate. The only factor is the activity coefficient γ. This must be understood as a nonideal factor that magnifies the ideal rate and expresses repulsion, because $\gamma > 1$ (cf. Figure 4 and eq 11). The observed change in the adsorption enthalpies and entropies (Figure 6 and Figure 7) supports the idea that the surface is a nonideal thermodynamic system. It has previously been mentioned[4,29] that a similar expression for the desorption rate can improve the prediction of thermal desorption data. The explanation is also in agreement with the models that assume quasi-equilibrium conditions with a constant sticking coefficient.[8]

It is worth noting that the unidirectional rates of adsorption or desorption increase exponentially as the temperature increases, while the amount of adsorbed molecules decreases. This may mean in practice that adsorption or desorption can be rate-limiting prior to a chemical or electrochemical reaction. This is relevant for carbon-based hydrogen storage[26] or for hydrogen reaction at electrochemical catalysts.[43,44] Our view that there is rapid transport of hydrogen along the graphite surface, is in agreement with results from, i.e., impedance spectroscopy on fuel cell anode materials.[43,44] In those experiments, such hydrogen transport was found indeed to be rate-limiting for the anode reaction.

Comparing Different Rate Expressions. A highly mobile hydrogen phase on the graphite surface also leads to a rapid equilibration within the adsorbed phase, meaning that it is reasonable to assume that there are quasi-equilibrium conditions of this phase, as proposed in ref 8. For these conditions, it further follows from our results that the sticking coefficient is constant at a given temperature.

Burress et al.[26] measured and simulated adsorption of hydrogen on graphite, exposing a bare surface to a gas pressure until saturation at 77 and 293 K. Their data were fitted to a Langmuir model, and they obtained good agreement with molecular dynamics results. Our results do not disagree with theirs. Using the expression for adsorption and desorption, eq 14, we estimated the rates of Burress et al. By integrating eq 14 over time under constant gas pressure, we obtained the adsorption time, t, needed to produce a certain surface coverage as

$$t = \frac{c^{\mathrm{sat}}(1-\theta_{\mathrm{eq}})^2}{k_{\mathrm{d}}}\left[\frac{\theta-\theta_i}{1-\theta_{\mathrm{eq}}} + \ln\left(\frac{\theta_i-\theta_{\mathrm{eq}}}{\theta-\theta_{\mathrm{eq}}}\right)\right] \quad (28)$$

In this equation, θ_i is the initial coverage, θ_{eq} is the final value of the surface coverage at $t = \infty$. This equation which is obtained for the whole domain of adsorption/desorption is very similar to the integrated empirical modified pseudo-first-order equation except for the sign of the linear term.[32,45] At long times and for small differences between the initial and final conditions, the logarithmic term dominates the kinetics, and we find the characteristic times for desorption or adsorption, t_{des} and t_{ads}:

$$t_{\mathrm{des}} = t_{\mathrm{ads}} = \frac{c^{\mathrm{sat}}(1-\theta_{\mathrm{eq}})^2}{k_{\mathrm{d}}} = 7.5\times10^{-13}(1-\theta_{\mathrm{eq}})^2\exp\left(\frac{4580\ \mathrm{J/mol}}{RT}\right) \quad (29)$$

The right-hand side term was obtained with the expressions of k_{d} and c^{sat}, eqs 25 and 27. Using this equation, at some distance from full coverage, we obtained characteristic times on the order of picoseconds, in agreement with the results reported by Burress et al.[26] At full coverage, eq 28 gives $t = 0$. This means that the pressure is infinite in the Langmuir model, or that the adsorption is infinitely fast, so this state must be avoided. Using constant gas pressure and constant temperature conditions, this model does not account for kinematics limitations due to homogenization of the physical conditions close to the surface.[11]

Despite fundamental criticisms about the construction of the model,[46] statistical rate theory is now gaining support for many purposes.[31,32,47,48] Statistical rate theory gives the same expressions for the equilibrium exchange rates as we obtain. Away from equilibrium, this theory cannot be reduced to the same unidirectional rates given by eq 6 (see the appendix). It should be possible to investigate this difference by further molecular dynamics simulations, as well as by experiments. This must be done for nonequilibrium states, however. It appears from the results that such work is of importance, given the importance of the field, and there is a need to establish a firm thermodynamic basis for kinetic phenomena, for input in reactor modeling at large.[49]

Conclusion

We have presented equilibrium molecular dynamics simulations of hydrogen adsorption on graphite. Below 170 K, we found that isotherms can be modeled with Langmuir isotherms, while at higher temperature, Henry's law applied. The isosteric adsorption enthalpies and entropies were calculated for different loadings. They showed a decrease as the loading increased, compatible with a nonideal surface behavior. These results are in good agreement with previous results from the literature. The observed adsorption and desorption rates were, however, not described by Langmuir kinetics in the system. We proposed a new set of rate equations where the adsorption rate is only proportional to the gas pressure and that the desorption rate is proportional to both the coverage and to the nonideal activity coefficient. These two unidirectional rates combine also at equilibrium to the Langmuir isotherm with the same equation for the Langmuir constant. This kinetic behavior is interpreted as the consequence of a mobile adsorbed phase. The effect may be important for fuel cell performance or hydrogen storage in carbonaceous materials.

APPENDIX

Net Rate of Adsorption from Statistical Rate theory. Ward and co-workers have over the last 20 years developed statistical rate theory for interfaces.[3−7,9,28,30] The adsorption−desorption process is expressed by

$$J = K_{\mathrm{e}}\left[\exp\left(\frac{\mu^{\mathrm{g}}-\mu^{\mathrm{s}}}{RT}\right) - \exp\left(\frac{\mu^{\mathrm{s}}-\mu^{\mathrm{g}}}{RT}\right)\right] \quad (A\text{-}1)$$

where K_{e} is the exchange rate between the gas phase and the surface under equilibrium conditions. This expression is given for microcanonical conditions, it slightly differs for open systems; see Panczyk[11] for more details.

Using eqs 6,7, and 8, we can write J as

$$J = J_{\mathrm{d}}\exp\left(\frac{\mu^{\mathrm{g}}-\mu^{\mathrm{s}}}{RT}\right) - J_{\mathrm{a}}\exp\left(\frac{\mu^{\mathrm{s}}-\mu^{\mathrm{g}}}{RT}\right) \quad (A\text{-}2)$$

J_{a} and J_{d} are related by

$$J_{\mathrm{a}} = J_{\mathrm{d}}\exp\left(\frac{\mu^{\mathrm{g}}-\mu^{\mathrm{s}}}{RT}\right) \quad (A\text{-}3)$$

At equilibrium, $J_{\mathrm{d}} = J_{\mathrm{a}}$. Away from equilibrium, J_{d} and J_{a} are different, so J from statistical rate theory must then differ significantly from our expression, eq A-2.

Acknowledgment. We are grateful to NFR for Storforsk grant no 167336/V30 and computer time from the NOTUR facilities.

References and Notes

(1) Guldberg, C. M.; Waage, P. *Forhandlinger: Videnskabs-Selskabet i Christiania* **1864**, *78*, 34.
(2) Eyring, H.; Eyring, E. *Modern Chemical Kinetics*; Chapman & Hall: London, 1965.
(3) Ward, C. A.; Rizk, M.; S., T. A. *J. Chem. Phys.* **1982**, *76*, 5606–5614.
(4) Ward, C. A.; Findlay, R. D. *J. Chem. Phys.* **1982**, *76*, 5615–5623.
(5) Findlay, R. D.; Ward, C. A. *J. Chem. Phys.* **1982**, *76*, 5624–5631.
(6) Elliott, J. A. W.; Ward, C. A. *J. Chem. Phys.* **1997**, *106*, 5667–5676.
(7) Ward, C. A.; Elliott, J. A. W. *J. Chem. Phys.* **1997**, *106*, 5677–5684.
(8) Kreuzer, H. J. *Langmuir* **1992**, *8*, 774–781.
(9) Rudzinski, W.; Borowiecki, T.; Panczyk, T.; Dominko, A. *J. Phys. Chem. B* **2000**, *104*, 1984–1997.
(10) Ho, Y. S.; Ng, J. C. Y.; McKay, G. *Sep. Purif. Methods* **2000**, *29*, 182–232.
(11) Panczyk, T. *Phys. Chem. Chem. Phys.* **2006**, *8*, 3782–3795.
(12) Ruthven, D. *Principles of adsorption and adsorption processes*; John Wiley & Sons: New York, 1984.
(13) Kreuzer, H. J.; Payne, S. *Surf. Sci.* **1988**, *198*, 235–262.
(14) Payne, S. H.; Kreuzer, H. J. *Surf. Sci.* **1988**, *205*, 153–176.

(15) Payne, S. H.; Kreuzer, H. J. *Surf. Sci.* **1989**, *222*, 404–429.
(16) Kreuzer, H. J.; Zhang, J. *Appl. Phys. A: Mater. Sci. Process.* **1990**, *51*, 183–190.
(17) Brenig, W.; Kreuzer, H. J.; Payne, S. H. *Phys. Rev. B* **2003**, *67*, 205419.
(18) Payne, S. H.; McEwen, J. S.; Kreuzer, H. J.; Menzel, D. *Surf. Sci.* **2005**, *594*, 240–262.
(19) de Groot, S. R.; Mazur, P. *Non-Equilibrium Thermodynamics*; Dover Publications: New York, 1984.
(20) Kjelstrup, S.; Bedeaux, D. *Non-Equilibrium Thermodynamics of Heterogeneous Systems*; Series on Advances in Statistical Mechanics, Vol. 16; World Scientific Publishing Co. Pte, Ltd., 2008.
(21) Pagonabarraga, I.; Rubi, J. M. *Physica A* **1992**, *188*, 553–567.
(22) Mayo, S. L.; Olafson, B. D.; Goddard, W. A. *J. Phys. Chem.* **1990**, *94*, 8897–8909.
(23) Nicholas, J. B.; Trouw, F. R.; Mertz, J. E.; Iton, L. E.; Hopfinger, A. J. *J. Phys. Chem.* **1993**, *97*, 4149–4163.
(24) van Duin, A. C. T.; Baas, J. M. A.; van de Graaf, B. *J. Chem. Soc., Faraday Trans.* **1994**, *90*, 2881–2895.
(25) Strobel, R.; Garche, J.; Moseley, P. T.; Jorissen, L.; Wolf, G. *J. Power Sources* **2006**, *159*, 781–801.
(26) Burress, J. W.; Kraus, M.; Beckner, M.; Cepel, R.; Suppes, G.; Wexler, C.; Pfeifer, P. *Nanotechnology* **2009**, *20*, 204026.
(27) Haas, O. E.; Simon, J. M.; Kjelstrup, S. *J. Phys. Chem. C* **2009**, *113*, 20281–20289.
(28) Ward, C. A.; Findlay, R. D.; Rizk, M. *J. Chem. Phys.* **1982**, *76*, 5599–5605.
(29) Gorte, R.; Schmidt, L. D. *Surf. Sci.* **1978**, *76*, 559–573.
(30) Rudzinski, W.; Plazinski, W. *J. Phys. Chem. B* **2006**, *110*, 16514–16525.
(31) Azizian, S.; Bashiri, H. *Langmuir* **2008**, *24*, 13013–13018.
(32) Azizian, S.; Bashiri, H. *Langmuir* **2008**, *24*, 11669–11676.
(33) Perry, R. H.; Green, D. W. *Perry's Chemical Engineers Handbook*; McGraw-Hill, 1997.
(34) Wyckoff, R. W. G. *Crystal Structures*; Interscience: New York, 1963.
(35) Allen, M. P.; Tildesly, D. J. *Computer Simulation of Liquids*; Claredon Press, Oxford, 1987.
(36) Anil Kumar, A. V.; Jobic, H.; Bhatia, S. K. *J. Phys. Chem. B* **2006**, *110*, 16666–16671.
(37) Benard, P.; Chahine, R. *Langmuir* **2001**, *17*, 1950–1955.
(38) Hirscher, M.; Panella, B. *J. Alloys Compd.* **2005**, *404*, 399–401.
(39) Panella, B.; Hirscher, M.; Roth, S. *Carbon* **2005**, *43*, 2209–2214.
(40) Zhou, L.; Zhou, Y.; Sun, Y. *Int. J. Hydrogen Energy* **2006**, *31*, 259–264.
(41) Thomas, J. M.; Thomas, W. J. *Principles and Practice of Heterogeneous Catalysis*; VCH Publishers Inc.: New York, 1997.
(42) Henriksen, N.; Hansen, F. *Theories of molecular reactions dynamics*; Oxford University Press: Oxford, 2008.
(43) Meland, A. K.; Kjelstrup, S.; Bedeaux, D. *J. Membr. Sci.* **2006**, *282*, 96–108.
(44) Paulus, U. A.; Veziridis, Z.; Schnyder, B.; Kuhnke, M.; Scherer, G. G.; Wokaun, A. *J. Electroanal. Chem.* **2003**, *541*, 77–91.
(45) Rudzinski, W.; Plazinski, W. *Langmuir* **2008**, *24*, 5393–5399.
(46) Zhdanov, V. P. *J. Chem. Phys.* **2001**, *114*, 4746–4748.
(47) Rudzinski, W.; Plazinski, W. *Langmuir* **2008**, *24*, 6738–6744.
(48) Pladzinski, W.; Rudzinski, W. *Langmuir* **2009**, *26*, 802–808.
(49) Froment, G. F.; Bischoff, K. *Chemical reactor analysis and design*; Wiley, 1990.

JP1011022